A REGIONAL FREQUENCY ANALYSIS OF UNITED KINGDOM EXTREME RAINFALL FROM 1961 TO 2000

H. J. FOWLER* and C. G. KILSBY

Water Resource Systems Research Laboratory, School of Civil Engineering and Geosciences, University of Newcastle upon Tyne, Newcastle upon Tyne, UK

ABSTRACT

Multi-day rainfall events are an important cause of recent severe flooding in the UK, and any change in the magnitude of such events may have severe impacts upon urban structures such as dams, urban drainage systems and flood defences and cause failures to occur. Regional pooling of 1-, 2-, 5- and 10-day annual maxima for 1961 to 2000 from 204 sites across the UK is used in a standard regional frequency analysis to produce generalized extreme value growth curves for long return-period rainfall events for each of nine defined climatological regions. Temporal changes in 1-, 2-, 5- and 10-day annual maxima are examined with L-moments using both a 10 year moving window and the fixed decades of 1961–70, 1971–80, 1981–90 and 1991–2000. A bootstrap technique is then used to assess uncertainty in the fitted decadal growth curves and to identify significant trends in both distribution parameters and quantile estimates.

There has been a two-part change in extreme rainfall event occurrence across the UK from 1961 to 2000. Little change is observed at 1 and 2 days duration, but significant decadal-level changes are seen in 5- and 10-day events in many regions. In the south of the UK, growth curves have flattened and 5- and 10-day annual maxima have decreased during the 1990s. However, in the north, the 10-day growth curve has steepened and annual maxima have risen during the 1990s. This is particularly evident in Scotland. The 50 year event in Scotland during 1961–90 has become an 8-year, 11-year and 25-year event in the East, South and North Scotland pooling regions respectively during the 1990s. In northern England the average recurrence interval has also halved. This may have severe implications for design and planning practices in flood control. Copyright © 2003 Royal Meteorological Society.

KEY WORDS: region; technique(s); climate variable(s); rainfall; extremes; flooding; climate change; recurrence interval

1. INTRODUCTION

The autumn and winter of 2000–01 provided the wettest months on record in the UK (Marsh, 2001) and widespread flooding throughout the last decade has enhanced the public concern that such heavy and prolonged rainfall events are a result of global warming. Analyses of rainfall trends in observed data (e.g. Bradley *et al.*, 1987; Diaz *et al.*, 1989; Groisman *et al.*, 1999) suggest a trend towards increased rainfall and enhanced variability in high latitudes of the Northern Hemisphere (e.g. Easterling *et al.*, 2000), particularly in winter. Significant positive trends in intensity have been observed in the UK (Osborn *et al.*, 2000; Lamb, 2001), Europe (Brunetti *et al.*, 2000; Frei and Schar, 2001) and worldwide (Iwashima and Yamamoto, 1993; Karl and Knight, 1998; Zhai *et al.*, 1999). These observations show agreement with the results of climate model integrations, which predict increases in both the frequency and intensity of heavy rainfall in the high latitudes under enhanced greenhouse conditions (e.g. Murphy and Mitchell, 1995; McGuffie *et al.*, 1999). The amplification of the global water cycle through global warming may have severe consequences in the UK, particularly in terms of increases in significant flood events.

---

* Correspondence to: H. J. Fowler, Water Resource Systems Research Laboratory, School of Civil Engineering and Geosciences, Cassie Building, University of Newcastle upon Tyne, Newcastle upon Tyne NE1 7RU, UK; e-mail: h.j.fowler@ncl.ac.uk

This study considers changes in extreme rainfall event frequency and intensity across the UK. An analysis of observed trends for the 1961–95 period by Osborn *et al.* (2000) indicates increases in the number of heavy rainfall days along with increases in the rainfall amount on those days, particularly in winter months. Additional analyses at three UK case-study locations by Lamb (2001) suggest that the frequency of longer duration extreme rainfalls has been increasing since the 1960s. These trends are supported by analysis of general circulation model (GCM) simulations and regional climate model (RCM) integrations. Palmer and Raisanen (2002) analysed 19 GCM simulations, and estimated that the probability of winter rainfall exceeding two standard deviations above normal will increase by factors of five and three respectively over northern and southern parts of the UK by 2100. RCM integrations over the period from 2080 to 2100 (Jones and Reid, 2001) also suggest that there will be dramatic increases in the heaviest rainfall events over Britain.

The observed increase in extreme rainfall has already caused severe impacts in both the UK and northern Europe, including major fluvial flooding (Lamb, 2001; Marsh, 2001) and landslides affecting rail networks, notably the East Coast line at Doncaster and fatal incidents in Scotland and northern England. A characteristic of these events has been their multi-day nature, with unremarkable 1 day totals (Lamb, 2001). These changes to the spatial and temporal distribution of extreme rainfall events in the UK are very important in the design of urban structures, such as drainage systems, dams, spillways and flood control measures, and may cause increased failure of such systems. Therefore, a re-evaluation of design estimates is needed.

In general, two approaches have been taken to assess rainfall extremes. The first approach uses a percentile or quantile method to assess extreme rainfall (e.g. Karl and Knight, 1998; Osborn *et al.*, 2000). In this approach, daily rainfall records are sorted and classes defined to contain a certain percentage of the total number of rainfall events for a season or month. Each of the classes contains an equal amount of total rainfall and can, therefore, be thought of as amount quantiles. The second approach uses statistical distributions to define extremes with given return periods on an annual basis (e.g. Hennesey *et al.*, 1997; McGuffie *et al.*, 1999). In this method, estimation of the magnitude of long return-period rainfall events involves fitting an extreme value distribution to the annual maxima (AM) series. This method produces return period estimates that are easily understood and can be used readily for design purposes.

In this study, a regional frequency analysis approach based on L-moments (Hosking and Wallis, 1997) is used to produce rainfall growth curves with an extreme value distribution. This involves the regional pooling of AM to allow the estimation of long return-period rainfall events when individual records are too short to allow their reliable estimation. Daily rainfall records from 204 sites across the UK for 1961–2000 are used to produce rainfall growth curves for 1-, 2-, 5- and 10-day AM series for each of the nine homogeneous rainfall regions defined by Wigley *et al.* (1984).

This method of pooling is also used to examine temporal variability in L-moment ratios and AM series, utilizing both a 10 year moving window and the fixed decades of 1961–70, 1971–80, 1981–90, and 1991–2000. This provides a comprehensive analysis of spatial and temporal changes in extreme rainfall event occurrence across the UK from 1961–2000.

2. OBSERVED RAINFALL DATA

The study has been limited, by necessity, to daily data, as sub-daily data are not generally available with sufficient coverage and length of record. However, daily data are adequate for the purposes of this study, since attention is focused on multi-day events.

Daily data for 110 stations (after Osborn *et al.* (2000)) for 1961–95 were updated using data from the British Atmospheric Data Centre (http://www.badc.rl.ac.uk/) to give complete records from 1961 to 2000. Additional sites were then chosen such that each of the nine regions defined by Wigley *et al.* (1984) in their study of UK rainfall contained at least 20 stations. These regions are defined in Figure 1 and were originally defined to take account of physiographic character and spatially coherent rainfall variability, based on an average of seven sites per region. This gave a total of 204 stations across the
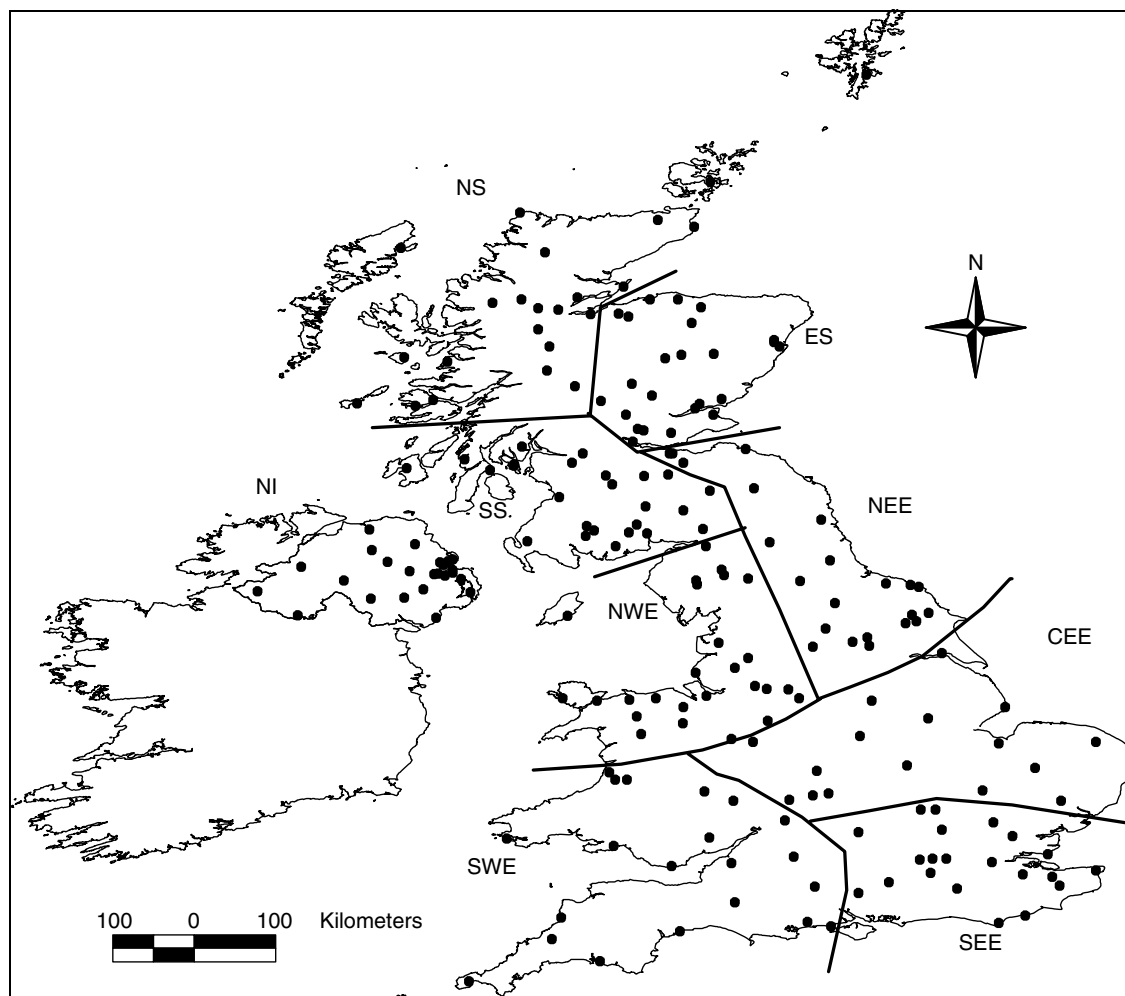
Figure 1. Location of the 204 UK daily rainfall records with complete or almost complete data for the 1961–2000 period and the nine coherent rainfall regions. The regions are: North Scotland (NS), East Scotland (ES), South Scotland (SS), Northern Ireland (NI), Northwest England (NWE), Northeast England (NEE), Central and Eastern England (CEE), Southeast England (SEE) and Southwest England (SWE)

UK chosen on the basis of record length and completeness, and to provide a good spatial coverage (see Figure 1).

3. REGIONALIZATION

Analyses were performed using L-moments of the AM series to determine whether the regions of Wigley *et al*. (1984) are appropriate for an analysis of extreme rainfall. Firstly, the three L-moment ratios L-CV, L-skewness and L-kurtosis were determined for the AM series at each site using a routine from Hosking (1997). Figure 2 shows a plot of L-CV against L-skewness for the mean values for each of the nine pooling regions. It can be seen that, generally, eastern regions display a greater L-CV value than western regions, suggesting higher variability in these regions. The highest L-skewness values are found in SWE and SEE. These fall as a move is made northwards, to much lower values in NS. In simple terms, this suggests that more intense rainfall events are experienced in southern regions of the UK. This is in line with the

accepted variation in rainfall growth curves as expressed in the regions of the Flood Studies Report (NERC, 1975).

A discordancy analysis was then performed to establish whether the distributions of site AM series within each region were acceptably similar. The discordancy measure D_i (Hosking and Wallis, 1997) compares the L-moment ratios of a site with those of the pooling group as a whole, hence identifying sites with L-moment ratios that are unusual relative to the pooling group. A high value of the discordancy measure indicates that a site may be discordant within the pooling group, but this may be caused by only a few unusual rainfall events. D_i is formally defined by Robson and Reed (1999): if M is the number of sites in the pooling group and $\boldsymbol{u}_i$ is a vector of the L-moment ratios at site i, then:

$$\boldsymbol{u}_i = (t_1, t_2, t_3)^T \tag{1}$$

where t_1 is L-CV, t_2 is L-skewness, t_3 is L-kurtosis and superscript T denotes the transpose of a vector. Thus, defining the two matrices $\boldsymbol{U}$ and $\boldsymbol{A}$ as

$$\boldsymbol{U} = \frac{1}{M} \sum_{i=1}^{M} \boldsymbol{u}_i \tag{2}$$

and

$$\boldsymbol{A} = \sum_{i=1}^{M} (\boldsymbol{u}_i - \boldsymbol{U})(\boldsymbol{u}_i - \boldsymbol{U})^T \tag{3}$$

the discordancy measure D_i for site i is then given by

$$D_i = \frac{1}{3} M (\boldsymbol{u}_i - \boldsymbol{U})^T \boldsymbol{A}^{-1} (\boldsymbol{u}_i - \boldsymbol{U}) \tag{4}$$

where $\boldsymbol{A}^{-1}$ is the inverse of matrix $\boldsymbol{A}$.
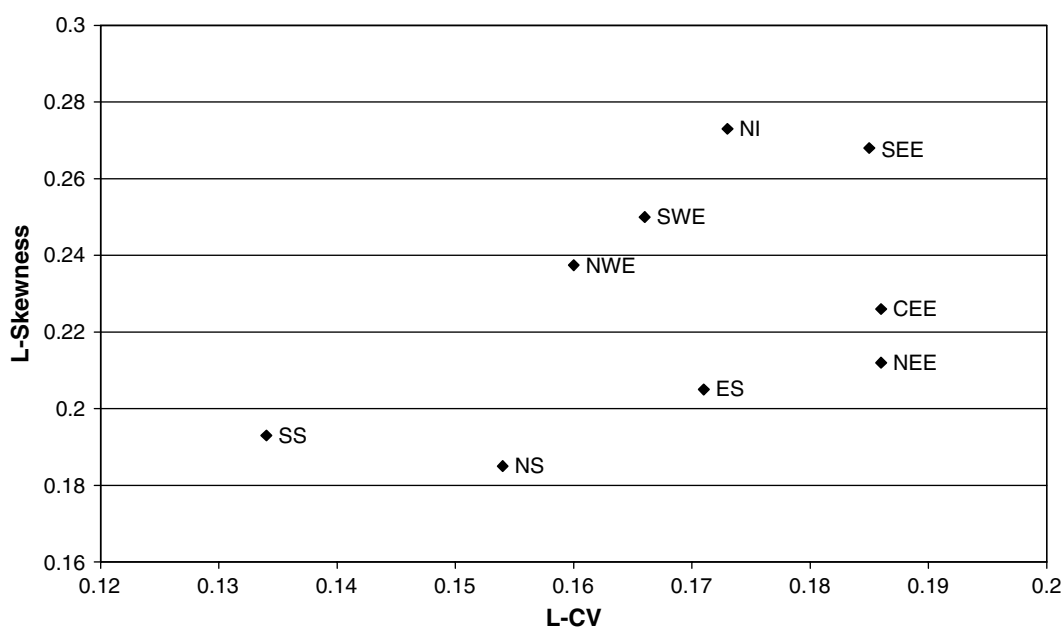

Figure 2. Comparison of mean L-CV and L-skewness in the nine regions

Critical values of the discordancy measure for each site in a pooling group based on a 10% significance level are suggested by Hosking and Wallis (1997). For a pooling group with more than 15 member sites, values of D_i higher than 3.0 show possible discordancy. Values of D_i greater than the critical value of 3 were only found for three sites. These were in the pooling regions of NEE and NWE.

In the NEE pooling region the two discordant sites, Lockwood Reservoir and Whitby Coastguard, have D_i values of 3.29 and 3.15 respectively. At Lockwood Reservoir, the high discordancy measure arises due to a single, unusually high rainfall event in 1976, when 104.6 mm fell in 24 h, and similarly at Whitby Coastguard. In the NWE pooling region, the site at Appleby is group discordant with a D_i of 3.06. At this site, again, the high discordancy measure results from a single, unusually high, AM. In this case, a heavy rainfall event on the 17 July 1983 produced 97.8 mm rainfall in 24 h. In each case, a single heavy rainfall event was found to have caused unusually high values of L-kurtosis, and so no adjustment to the pooling groups was considered necessary.

4. REGIONAL FREQUENCY ANALYSIS

4.1. Methodology

A regional frequency analysis approach based on L-moment methods (Hosking and Wallis, 1997) was taken to generate rainfall growth curves for 1-, 2-, 5- and 10-day events for each of the nine regions. For each site, annual rainfall maxima for 1-, 2-, 5- and 10-day events are standardized using the median event (RMED), calculated using data from the period 1961–90. This removes site-specific factors from the regional analysis and is the same variable as that used in the FORGEX (Focused Rainfall Growth Extension) method (Reed *et al.*, 1999) of the Flood Estimation Handbook (FEH) (IH, 1999). L-moment ratios derived from single site analyses within a region are then combined by regional averaging, weighted according to record length (see Hosking and Wallis (1997)). Thus, giving an example formula for L-CV

$$\text{L-CV}_{pooled} = \sum_{i=1}^{N} w_i \text{L-CV}_i \tag{5}$$

where N is the number of sites in the pooling group and the weight w_i is an effective record length at the ith site defined by

$$w_i = \frac{n_i}{\sum_{i=1}^{N} n_i} \tag{6}$$

The denominator is the total number of station-years of record in the pooling group, and the numerator is the number of station-years at the ith site. The weighted average L-skewness and L-kurtosis moment ratios are derived in the same way. The station-year approach to estimating long return-period events is avoided, as this assumes that site records are mutually independent; this is only valid for very widely scattered sites and thus is unjustified in this application.

The classical L-moments approach is then used to fit the generalized extreme value (GEV) distribution for each AM series by matching the sample L-moments to the distribution L-moments. The GEV distribution is widely used in extreme event frequency analysis in the UK (e.g. FEH) and is used in preference to the Gumbel distribution, as the literature increasingly suggests that the distribution of extreme events may be more heavily tailed.

The changing shape of the standardized AM series as it moves from 1-day to 10-day rainfall totals and a comparison of the shape of the unfitted distributions between different regional pooling groups can be seen in Figure 3. Although most of the growth curves approximate a straight line, and therefore the Gumbel distribution, others have significant curvature. This is particularly apparent in the SEE region, where the 1-, 5- and 10-day AM series are significantly curved, and justifies the choice of the GEV distribution in fitting. The curvature is also evident to a lesser extent in the 10-day AM series of both the SWE and NS pooling
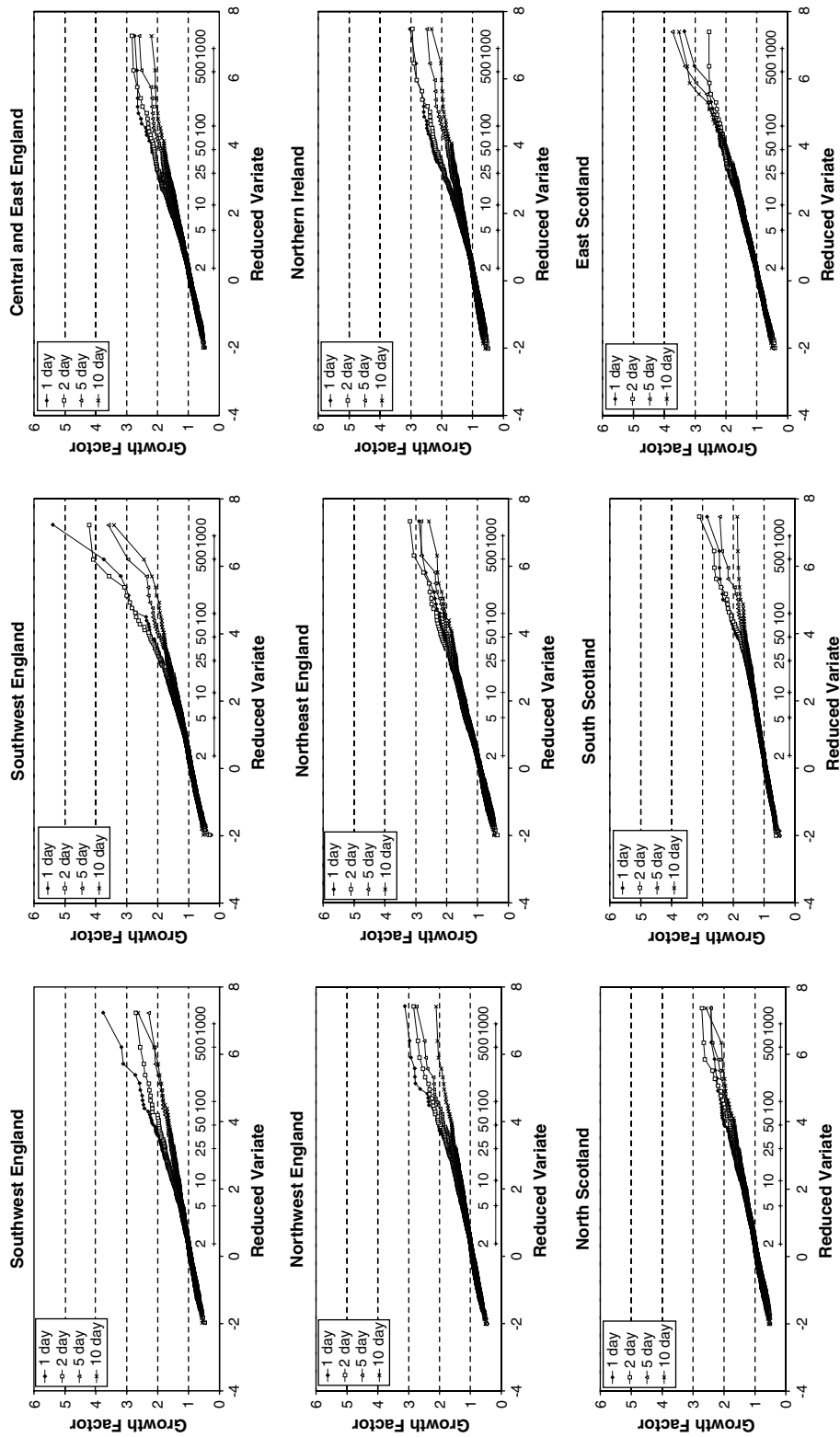
Figure 3. Shape of standardized annual maximum distributions for the nine pooling regions

regions and is possibly due to the existence of two mechanisms of rainfall; frontal (flat) and convective (curved upper section). It can be observed that, for 10-day totals in particular, many of the AM distributions exhibit significant curvature. This is especially prevalent in the south of England and may be important in the prediction of future rainfall extremes.

The GEV distribution has three parameters and is described by

$$x(F) = \xi + \frac{\alpha}{k} \left[1 - (-\ln F)^k \right] \qquad (k \neq 0) \tag{7}$$

where ξ is the location parameter, α the scale parameter, k the shape parameter and F refers to a given quantile.

A growth curve was fitted for each AM series using the regionally averaged site L-moment ratios. The fitted growth curve is given by

$$x(F) = 1 + \frac{\beta}{k} \left[(\ln 2)^k - (-\ln F)^k \right]$$

where

$$\beta = \frac{\alpha}{\xi + \frac{\alpha}{k} \left[1 - (\ln 2)^k \right]} \tag{8}$$

The parameter k is estimated from the L-skewness (Hosking *et al.*, 1985)

$$k \approx 7.8590c + 2.9554c^2$$

where

$$c = \frac{2}{3 + t_3} - \frac{\ln 2}{\ln 3} \tag{9}$$

The parameter β is estimated using L-CV (Hosking and Wallis, 1997) as

$$\beta = \frac{kt_2}{t_2 \left[\Gamma(1 + k) - (\ln 2)^k \right] + \Gamma(1 + k)(1 - 2^{-k})} \tag{10}$$

where Γ denotes the gamma function, t_2 is the L-CV L-moment ratio and t_3 is the L-skewness L-moment ratio.

The fitted distribution plotting positions on a variate versus Gumbel reduced variate plot are determined according to the Gringorten (1963) formulae:

$$F_i = \frac{i + 0.44}{N + 0.12} \tag{11}$$

where F_i is the non-exceedance probability, i the rank in increasing order, and N the number of AM in the pool. The Gumbel reduced variate is defined by

$$y = -\ln(-\ln F_i) \tag{12}$$

The fitted growth curves are shown in Figure 4. Figure 5 gives an approximation of the pooled AM rainfall in millimetres by using the geometric mean RMED of all stations in the pooling group for a particular event duration during the period 1961–90 as a multiplier in each case. Fitted GEV distribution parameters for the nine regions can be found in Table I. Although return periods up to 1000 years are shown in Figures 3 to 5, we do not suggest that return period estimates above 50 years are used in impact studies.
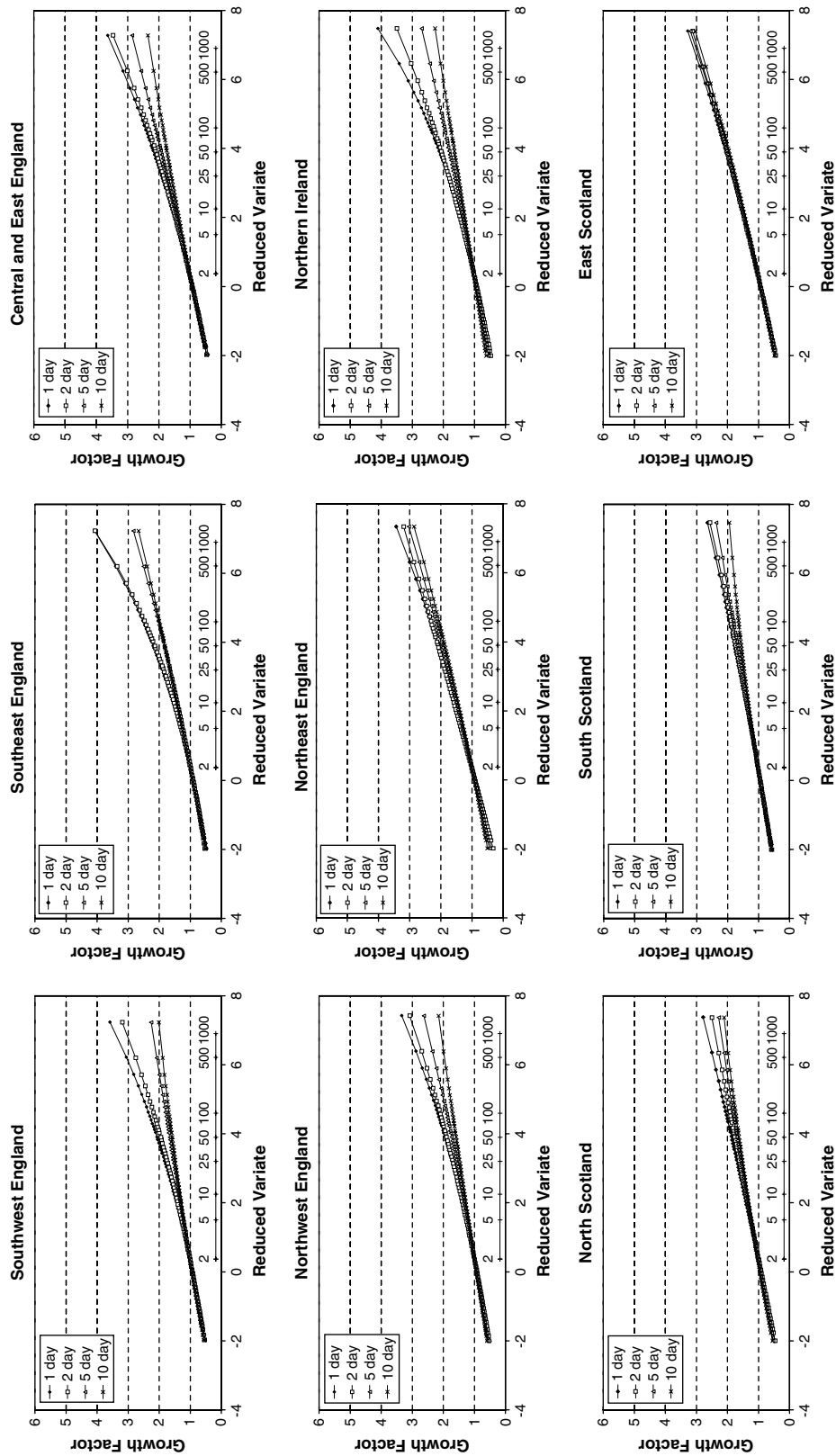
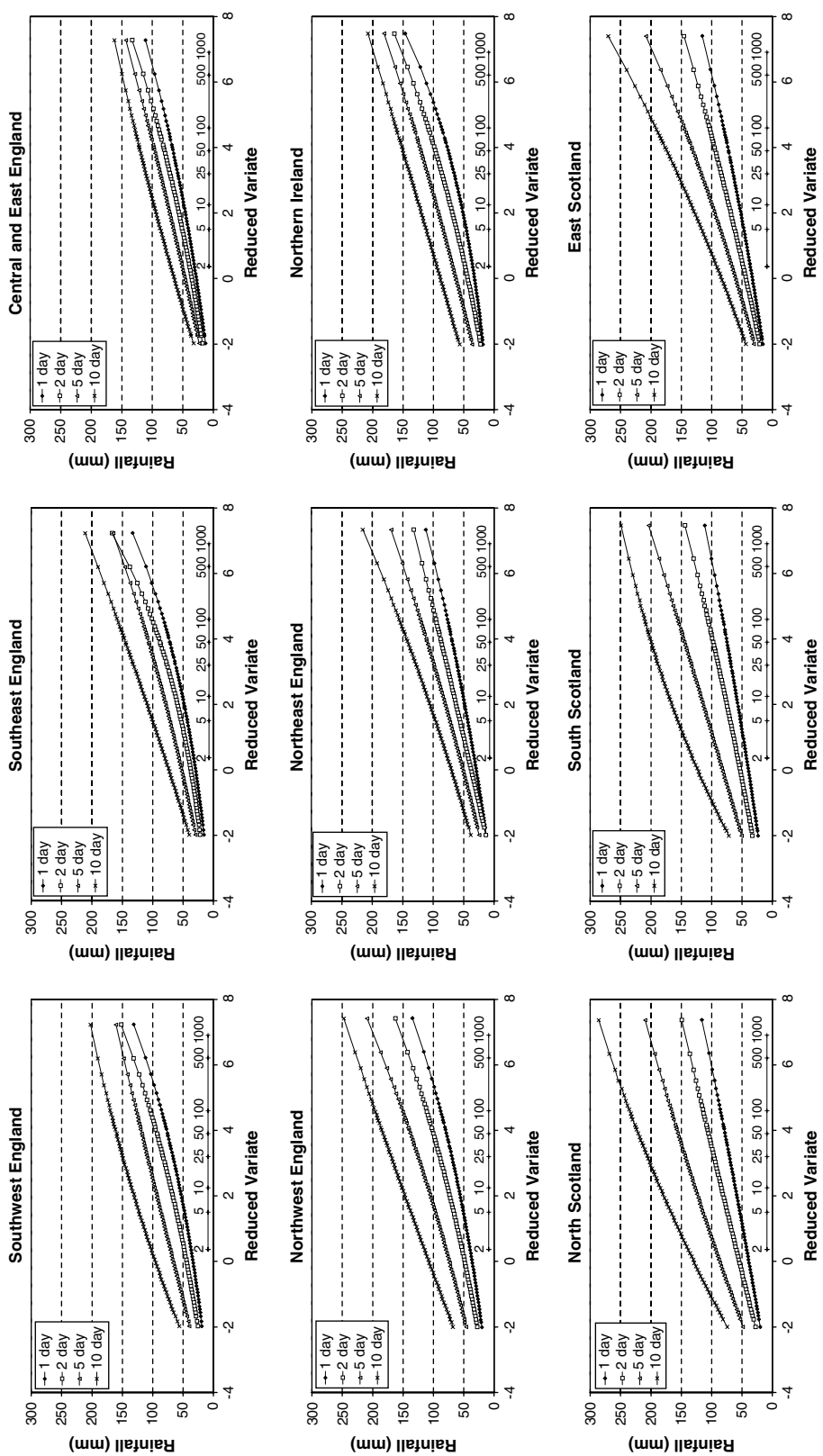Figure 4. Fitted standardized annual maximum GEV distributions for the nine regions

Figure 5. Fitted annual maximum GEV distributions for the nine pooling regions (using mean regional RMED for 1961–90 as a multiplier)

4.2. Estimating uncertainty

An estimate of uncertainty in return-period predictions of the pooled growth curve gives some confidence in the use of the growth curve for design purposes. Two methods have been used in this analysis. The first, the pooled uncertainty measure (PUM; Robson and Reed, 1999), addresses the variation in growth curves within a region. The PUM is a weighted average of the differences between each site growth factor and the pooled growth factor measured on a logarithmic scale. The pooled uncertainty measure for return period T, PUM_T, is defined by (Robson and Reed, 1999)

$$\mathrm{PUM}_T = \sqrt{\frac{\sum_{i=1}^{N} n_i (\ln x_{T_i} - \ln x_{T_i}^P)^2}{\sum_{i=1}^{N} n_i}} \tag{13}$$

where N is the number of sites in the pool, n_i is the record length in years of the ith site, x_{T_i} is the T-year growth factor for the ith site, and $x_{T_i}^P$ is the T-year pooled growth factor for the ith site.

The PUM_T for $T = 2, 5, 10, 25,$ and 50 can be found in Table II, reflecting the average uncertainty in the T-year growth factor at each return period. An estimate of the regional average uncertainty in millimetres is given by multiplying by the regional mean RMED in each case. The uncertainties are small, suggesting coherent pools, with typical values of PUM ranging from 6 mm for 1-day 50 year events up to 12 mm for 10-day 50 year events. The design storm can thus be estimated for 1-, 2-, 5- and 10-day rainfall totals for any part of the UK by using the correct regional growth curve and multiplying by the station RMED. To allow for uncertainty in the pooled growth curve, the appropriate PUM_T should be multiplied by the station RMED and then added to the previous design storm estimate.

The second measure allows for the effect of spatial dependence, where single major storm events give rise to AM at several sites in the same region. A bootstrap method (Efron, 1979) was used, where one year of record at a time was removed from the pooled regional data and the growth curve refitted for each decade. This gave uncertainty limits around the growth curves for each region that are larger than those derived using the PUM. The combined uncertainty envelope is then plotted for each growth curve.

5. ESTIMATING TEMPORAL CHANGE IN EXTREME RAINFALL

5.1. Methodology

Changes in the regional growth curve parameters and L-moment ratios during the period from 1961 to 2000 were examined using a 10 year moving window. For each of the 204 sites, annual maxima are found for 1-, 2-, 5- and 10-day rainfall totals. If the ith AM rainfall amount at site j during decade k is denoted by P_{ijk}, then the standardized AM are defined as (after Reed *et al.* (1999))

$$X_{ijk} = \frac{P_{ijk}}{\mathrm{RMED}_{jk}} \tag{14}$$

where RMED_{jk} denotes the median of annual maxima at site j during decade k. For each decade in a moving 10 year window from 1961 to 2000, the L-moment ratios were determined using a routine from Hosking (1997) and examined for trends.

Further analysis was undertaken by splitting the records into four separate decades, 1961–70, 1971–80, 1981–90 and 1991–2000, and standardizing by RMED as before. For each region, the standardized AM data are then pooled for each separate decade and GEV distributions fitted. Finally, each annual maximum is

Table I. Fitted GEV parameters and L-moment ratios for the nine pooling regions using data for 1961–2000

Pooling region	Duration (days)	GEV parameters			L-moment ratios		
		ξ	α	k	L-CV	L-skewness	L-kurtosis
SWE	1	0.921	0.231	−0.121	0.166	0.250	0.178
	2	0.933	0.216	−0.096	0.153	0.233	0.181
	5	0.937	0.191	0.011	0.125	0.163	0.167
	10	0.951	0.185	0.068	0.116	0.127	0.143
SEE	1	0.897	0.247	−0.147	0.185	0.268	0.207
	2	0.912	0.224	−0.169	0.172	0.283	0.226
	5	0.905	0.21	−0.063	0.149	0.211	0.185
	10	0.924	0.22	−0.023	0.148	0.185	0.166
CEE	1	0.918	0.27	−0.085	0.186	0.226	0.169
	2	0.932	0.252	−0.085	0.172	0.226	0.160
	5	0.943	0.243	−0.022	0.158	0.184	0.130
	10	0.932	0.222	0.038	0.142	0.146	0.128
NWE	1	0.899	0.218	−0.103	0.160	0.238	0.183
	2	0.923	0.213	−0.079	0.150	0.222	0.170
	5	0.933	0.185	−0.055	0.129	0.206	0.190
	10	0.935	0.172	0.012	0.114	0.162	0.188
NEE	1	0.897	0.27	−0.064	0.186	0.212	0.155
	2	0.915	0.296	−0.014	0.190	0.179	0.138
	5	0.925	0.251	−0.036	0.167	0.193	0.155
	10	0.931	0.223	−0.043	0.150	0.198	0.140
NI	1	0.905	0.228	−0.154	0.173	0.273	0.193
	2	0.929	0.245	−0.085	0.170	0.226	0.163
	5	0.947	0.207	−0.033	0.138	0.191	0.129
	10	0.965	0.171	−0.006	0.112	0.174	0.147
NS	1	0.927	0.23	−0.023	0.154	0.185	0.158
	2	0.917	0.221	0.008	0.146	0.165	0.166
	5	0.949	0.204	0.034	0.129	0.148	0.168
	10	0.955	0.193	0.057	0.120	0.134	0.151
SS	1	0.943	0.199	−0.036	0.134	0.193	0.162
	2	0.951	0.188	−0.037	0.127	0.194	0.193
	5	0.962	0.184	−0.006	0.120	0.174	0.168
	10	0.963	0.183	0.092	0.111	0.112	0.143
ES	1	0.937	0.256	−0.054	0.171	0.205	0.175
	2	0.94	0.255	−0.037	0.156	0.179	0.137
	5	0.938	0.246	−0.054	0.164	0.205	0.156
	10	0.94	0.235	−0.045	0.157	0.199	0.176

multiplied by the mean RMED of all stations in that pool for that decade, i.e.

$$\hat{P}_{ijk} = X_{ijk} \sum_{j=1}^{j=n} \text{RMED}_{jk} \Big/ n \qquad (15)$$

where $\hat{P}_{ijk}$ gives an approximation of the pooled AM rainfall in millimetres.

5.2. Change in L-moment ratios

The L-moment ratios are a direct measure of the AM distribution and, as such, provide a better illustration of changes than fitted GEV parameters themselves. Figure 6 shows the variation and trend in L-moment ratios

Table II. PUM values for each rainfall duration and each of the nine regions. Also given are the estimates of the regional PUM in millimetres for the return period (i.e. PUM multiplied by regional mean RMED)

| Duration	Return period (years)	SWE		SEE		CEE		NWE		NEE		NI		NS		SS		ES	
		PUM	Regional PUM (mm)	PUM	Regional PUM (mm)	PUM	Regional PUM (mm)	PUM	Regional PUM (mm)	PUM	Regional PUM (mm)	PUM	Regional PUM (mm)	PUM	Regional PUM (mm)	PUM	Regional PUM (mm)	PUM	Regional PUM (mm)
1-day	2	0.04	1.5	0.03	0.8	0.03	0.9	0.05	1.8	0.04	1.4	0.05	1.7	0.04	1.6	0.04	1.6	0.04	1.5
	5	0.06	2.2	0.05	1.6	0.05	1.5	0.07	2.7	0.05	1.7	0.07	2.5	0.06	2.3	0.05	2.2	0.05	1.9
	10	0.08	3.1	0.08	2.6	0.07	2.3	0.09	3.7	0.06	1.9	0.09	3.2	0.08	3.2	0.07	3.0	0.08	2.8
	25	0.13	4.9	0.13	4.4	0.11	3.5	0.13	5.4	0.07	2.3	0.12	4.3	0.11	4.7	0.10	4.4	0.12	4.1
	50	0.18	6.6	0.19	6.1	0.15	4.5	0.17	7.0	0.09	2.9	0.15	5.5	0.14	6.0	0.13	5.7	0.16	5.5
2-day	2	0.04	1.8	0.04	1.5	0.04	1.5	0.04	2.1	0.05	2.0	0.04	2.0	0.04	2.6	0.03	1.6	0.05	2.1
	5	0.06	2.6	0.06	2.4	0.07	2.7	0.06	3.2	0.06	2.6	0.07	3.4	0.07	4.0	0.04	2.2	0.06	2.9
	10	0.07	3.4	0.09	3.8	0.10	3.7	0.09	4.5	0.08	3.2	0.10	4.9	0.09	5.5	0.06	3.3	0.08	3.8
	25	0.10	4.7	0.16	6.4	0.14	5.3	0.13	6.9	0.11	4.5	0.15	7.2	0.13	8.0	0.10	5.4	0.12	5.6
	50	0.13	6.0	0.22	8.9	0.17	6.7	0.17	9.1	0.14	5.6	0.20	9.3	0.17	10.0	0.13	7.4	0.14	6.8
5-day	2	0.03	2.4	0.03	1.9	0.03	1.5	0.03	2.4	0.04	2.0	0.03	2.1	0.04	3.8	0.03	2.5	0.04	2.5
	5	0.05	3.7	0.04	2.5	0.05	2.5	0.05	4.1	0.06	3.2	0.06	3.8	0.07	6.3	0.04	3.2	0.05	3.5
	10	0.08	5.3	0.07	4.2	0.07	3.6	0.08	6.0	0.08	4.3	0.08	5.6	0.09	8.4	0.05	4.3	0.08	5.4
	25	0.11	7.9	0.12	7.0	0.10	5.2	0.12	9.3	0.11	6.0	0.12	8.2	0.13	12.2	0.08	6.5	0.13	8.8
	50	0.14	10.0	0.16	9.5	0.13	6.7	0.16	12.3	0.13	7.5	0.16	10.5	0.16	14.9	0.10	8.7	0.17	11.3
10-day	2	0.04	3.8	0.04	3.0	0.03	2.1	0.02	2.5	0.04	2.9	0.03	2.4	0.04	4.8	0.02	2.2	0.03	2.9
	5	0.05	5.2	0.04	3.4	0.05	3.5	0.03	3.7	0.06	4.8	0.05	4.3	0.06	8.1	0.03	4.4	0.05	4.8
	10	0.07	6.6	0.06	4.8	0.07	4.8	0.05	5.5	0.08	6.1	0.07	6.2	0.08	11.1	0.05	6.2	0.08	7.1
	25	0.10	9.7	0.09	7.4	0.10	6.8	0.08	9.0	0.10	7.8	0.10	8.9	0.12	15.8	0.07	9.2	0.13	11.3
	50	0.12	12.5	0.13	10.2	0.12	8.4	0.11	12.5	0.12	9.3	0.13	11.5	0.14	19.2	0.09	11.5	0.16	14.1
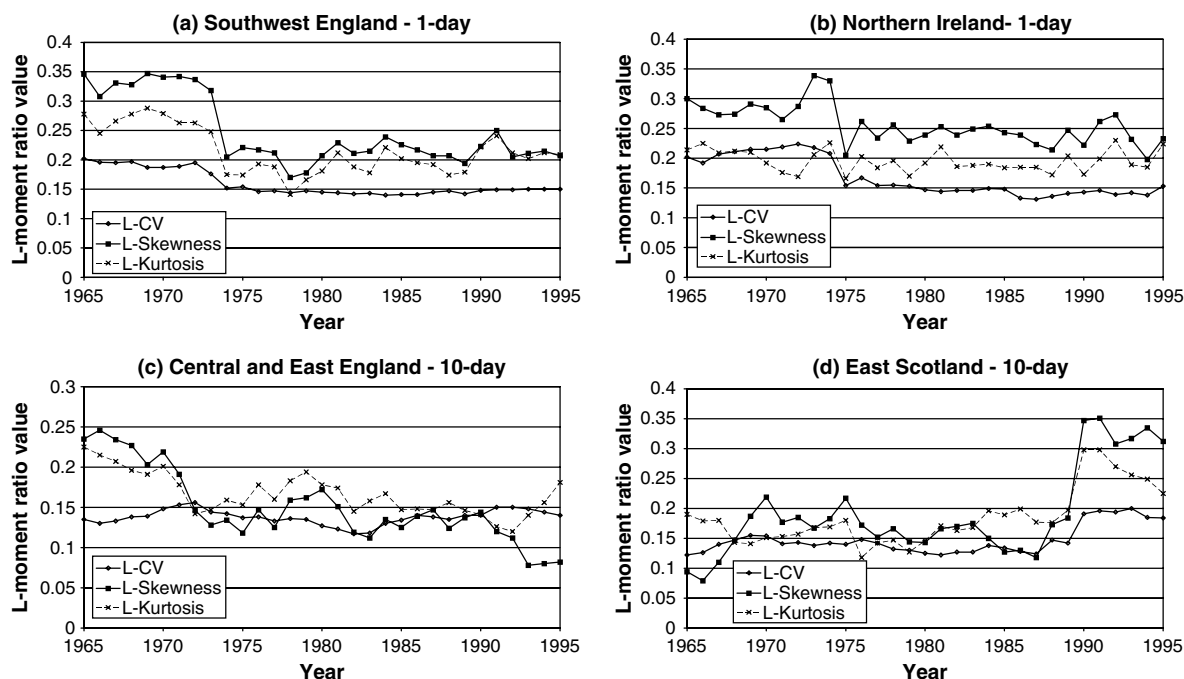
Figure 6. Changing L-moment ratios for 1961–2000: (a) SWE region, 1-day; (b) NI region, 1-day; (c) CEE region, 10-day; (d) ES region, 10-day

for regions and durations where the change is the most significant. Results indicate that firstly, at 1 and 2 day durations, there has been a shift in some western regions to lower L-moment ratios from 1961 to 2000. This is especially prevalent in the SWE and NI pooling regions (Figure 6(a) and (b)). However, this change is not seen in other western regions, such as NWE and NS. Secondly, at 5 and 10 days duration, in particular 10 days, there is a two-part shift across the UK. In northern and western regions (NS, SS, ES, NWE and NI) there has been a move to higher L-moment ratios, particularly in ES (see Figure 6(d)). In southern and eastern regions (CEE, NEE, SEE and SWE), L-moment ratios have been declining throughout the period, and especially in the most recent decade (see Figure 6(c)).

In simple terms this represents a change in extreme rainfall properties, with increased variability (rising L-CV) and increased intensity (rising L-skewness) of 5- and 10-day rainfall events in northern and western regions, and the opposite change occurring in southern and eastern parts of the UK. A similar shift in western regions indicates decreased variability in the 1-day rainfall event.

5.3. Change in growth curve shape

The shape of the fitted GEV distribution has changed over the last 40 years in some regions. These changes are markedly different between the south and north of the UK and are mainly seen at 5 and 10 days duration.

In the SEE, SWE and CEE pooling regions the growth curve has become flatter over the last decade from 1991 to 2000. This can be seen in the 5- and 10-day rainfall annual maxima, particularly in the SEE pooling region. Growth curves for 10 days duration in SEE and SWE are shown in Figure 7(a) and (b) respectively, along with their uncertainty estimates. These overlap, hence the change cannot be considered significant. In the NEE and NWE pooling regions the opposite change occurs, with the growth curve increasing in gradient for 5- and 10-day rainfall annual maxima. Growth curves for the 10-day duration in the NEE and NWE regions are shown in Figure 7(c) and (d) respectively. Uncertainty limits show that the changes are not significant.

In Scotland, dramatic changes in the shape of the growth curve occur in the east. In ES (Figure 8) the growth curve steepens markedly at all durations and for all decades. These changes are significant as the uncertainty limits are clearly separated from the growth curves in previous decades, particularly for the 5-day
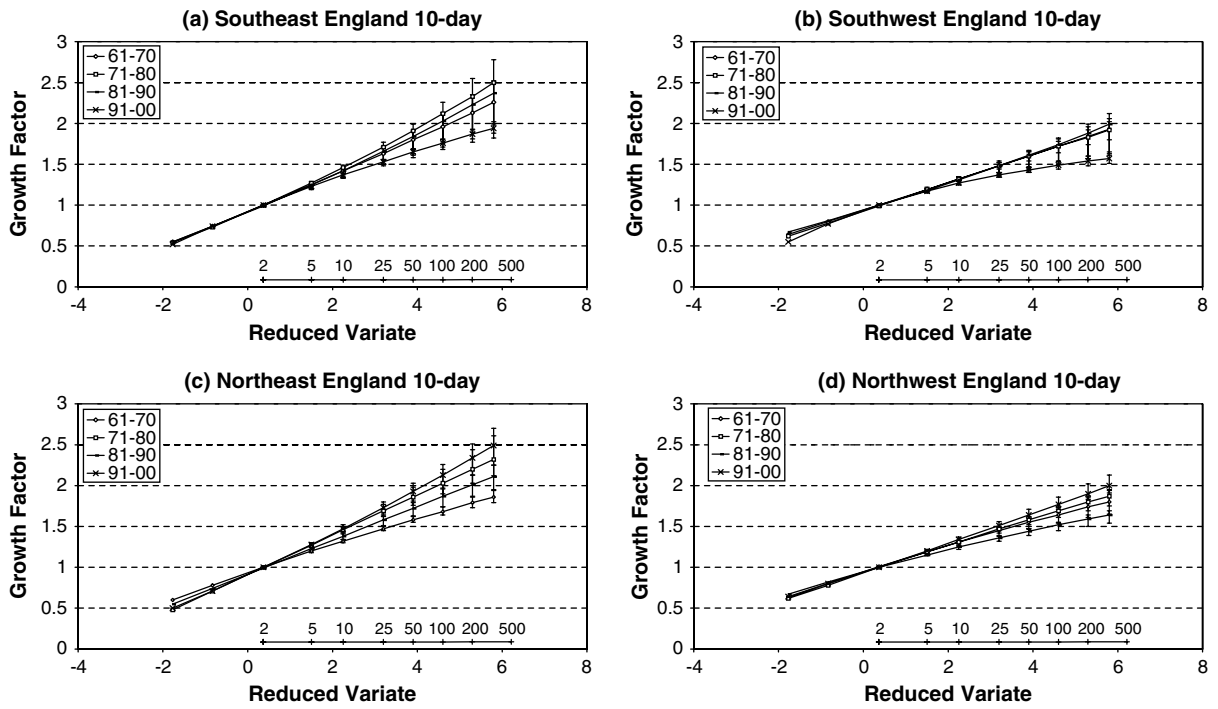
Figure 7. Decadal change in the 10-day growth curve: (a) SEE; (b) SWE; (c) NEE; (d) NWE
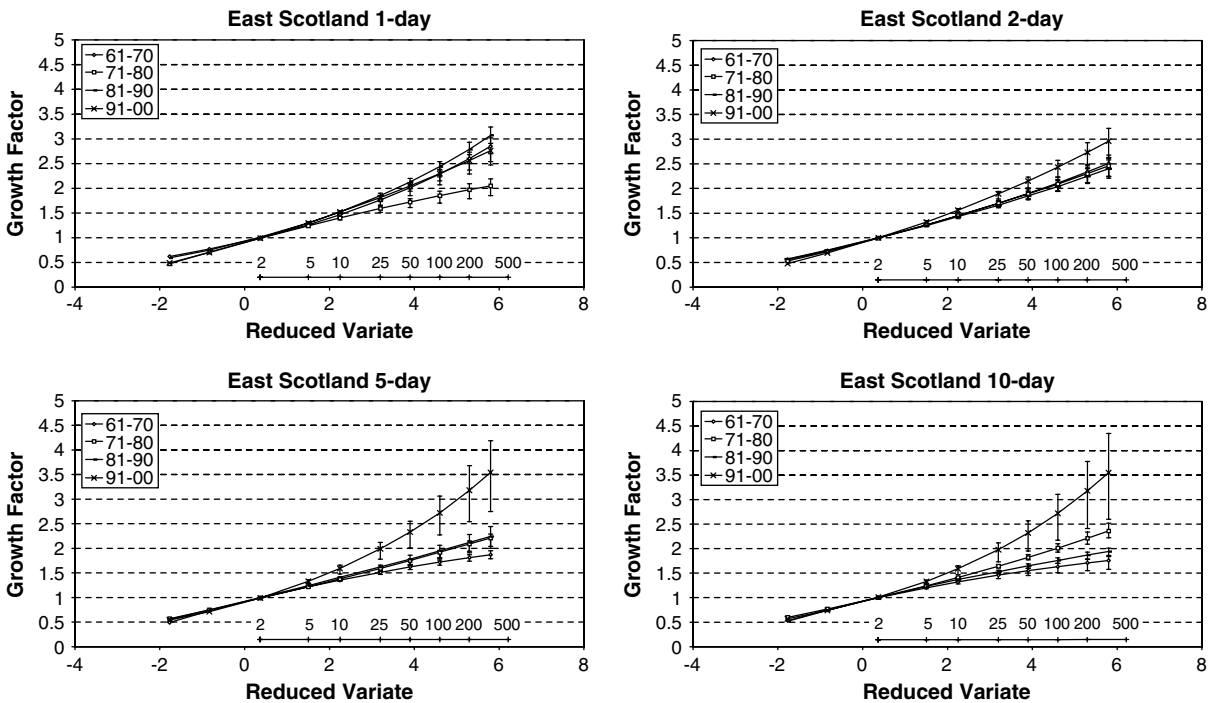

Figure 8. Decadal change in the 1-, 2-, 5- and 10-day growth curves in the ES pooling region

duration (significant for all return period estimates) and the 10-day duration (significant above the 10-year return period estimate). In the NS and SS pooling regions (not shown), however, there has been little change in the shape of the distribution over the last 40 years.

5.4. Change in magnitude of annual maxima (RMED)

Table III gives mean RMED values for each pooling region at each duration and for each decade. It can be seen that, in general, and particularly in the north and west of the UK, the 1980s and 1990s have seen a

Table III. Mean RMED per decade for the nine pooling regions for durations of: (a) 1 day; (b) 2 days; (c) 5 days; (d) 10 days. The highest value of decadal RMED is shown in bold

Pooling region	1961–70	1971–80	1981–90	1991–2000
(a)				
SWE	**41.4**	40.3	37.7	39.1
SEE	36.9	**37.2**	32.2	33.5
CEE	34.3	32.8	32.1	**34.6**
NWE	42.8	**43.4**	42.3	41.0
NEE	34.5	34.2	**36.8**	34.3
NI	**42.4**	36.2	38.2	36.6
NS	44.1	42.2	**47.2**	45.1
SS	44.1	42.9	44.3	**47.7**
ES	37.6	33.8	40.5	**42.1**
(b)				
SWE	51.9	**53.0**	49.2	52.0
SEE	**48.6**	45.5	41.4	41.1
CEE	41.9	40.9	41.5	**44.1**
NWE	57.0	**57.6**	55.1	55.3
NEE	42.9	44.1	**46.9**	45.7
NI	**54.2**	48.8	51.6	51.0
NS	61.5	58.7	**65.6**	63.8
SS	58.2	56.7	60.0	**63.9**
ES	49.8	47.3	50.6	**56.7**
(c)				
SWE	71.2	74.4	75.1	**76.6**
SEE	62.1	**62.2**	58.8	58.0
CEE	52.6	54.6	53.7	**57.3**
NWE	82.8	82.9	81.4	**86.2**
NEE	56.7	59.9	60.9	**62.9**
NI	73.9	68.5	69.8	**75.8**
NS	90.9	91.0	**105.3**	102.4
SS	87.6	83.2	95.4	**101.4**
ES	67.9	63.6	70.7	**82.7**
(d)				
SWE	101.2	103.1	107.6	**108.2**
SEE	82.5	84.5	**85.0**	82.0
CEE	70.2	73.8	71.8	**74.3**
NWE	118.5	115.8	116.4	**120.8**
NEE	76.4	82.1	80.1	**83.0**
NI	96.1	94.0	97.4	**103.0**
NS	130.6	134.9	151.7	**152.2**
SS	126.8	122.4	141.6	**147.0**
ES	91.9	86.3	96.8	**110.5**

changing RMED, with a shift upwards in most cases. This is especially obvious for 5- and 10-day rainfall events, where 1991–2000 shows the highest mean RMED for a 10-day event in every region excepting SEE, suggesting that it is at longer durations that change is occurring. This is most prominent in Scotland. In SS and ES the highest mean RMED values for all durations occur during the decade from 1991 to 2000.

In southern and central England, recent events during the 1980s and 1990s have been less extreme than events during the 1960s and 1970s. The AM series for SWE, SEE and CEE reveal many extreme events in the 1960s and 1970s. The decade from 1961 to 1970 was, in fact, highly unusual: the period 1961–64 was extremely dry across the UK, but thereafter it was extremely wet. These two extremes of dry and wet, found in the same decade, may account for the unusual shape of the growth curve found in both the regions of SWE and NI (Figure 9(a) and (b)) during the 1960s.

Unusually high AM during the 1960s and 1970s can particularly be seen in the AM series for the SEE region (Figure 9(c) and (d)). The largest AM during the decade from 1961 to 1970 occurs in 1968. In the 1960s, high 2-day AM and smaller 1-day AM are associated with the event of the 14–15 September 1968. During the 1970s, there are high AM in 1973. These are related to a single event on the 20 September and provide very large 1-day rainfall totals at some sites. At Manston (Kent), for example, there was 160.8 mm rainfall, 5.6 times larger than the decadal site median. Rainfall approximating 100 mm also occurred at Boxley (Kent), 102.1 mm, Faversham (Kent), 99.1 mm, and Wye (Kent), 127.5 mm.

Although in southern and central England recent rainfall events have been less extreme than events during the 1960s and 1970s, in the rest of the nine regions defined by Wigley *et al.* (1984) a different picture emerges. In northern regions there has been a move towards increasing extremes in recent years. Nowhere is this more prominent than in ES.

In ES the growth curve during the 1990s provides a dramatic departure from the growth curve during the previous decades, and is enhanced considerably by the increase in *RMED* (see Figure 10). This is particularly apparent for the 5- and 10-day growth curves, due to a large increase in extreme rainfall events during the 1990s. This increase can be substantially explained by rainfall events during September 1995 and October 1993.
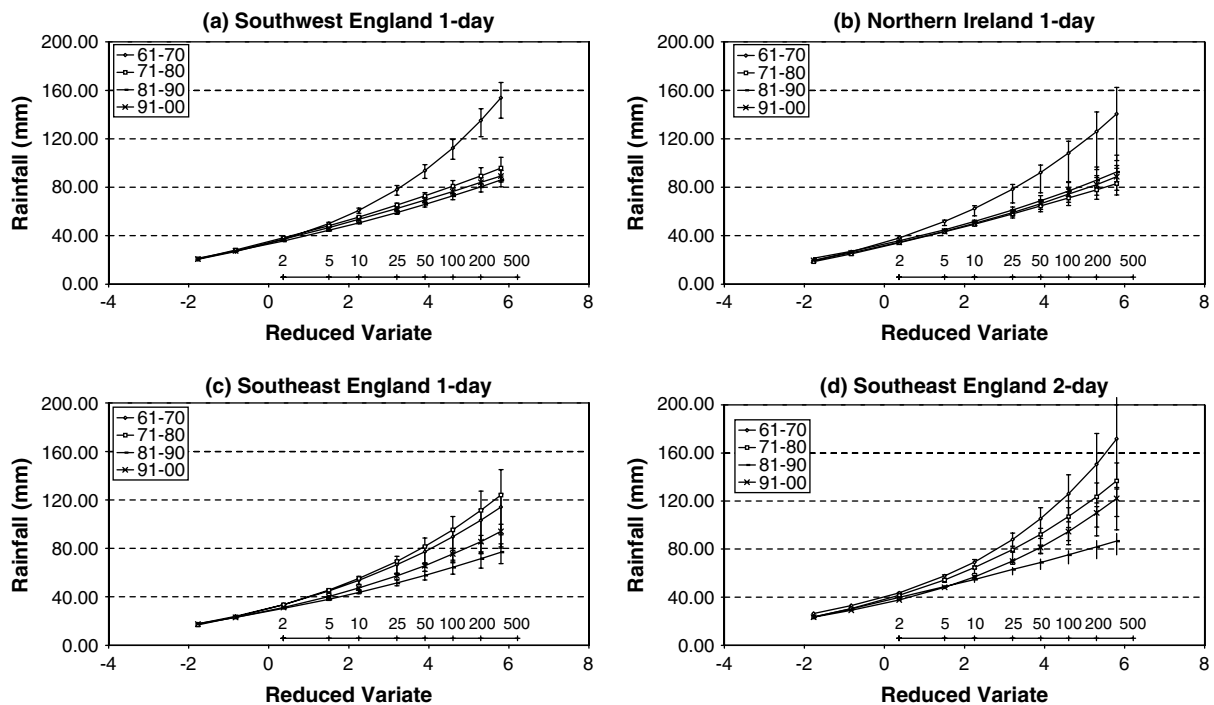

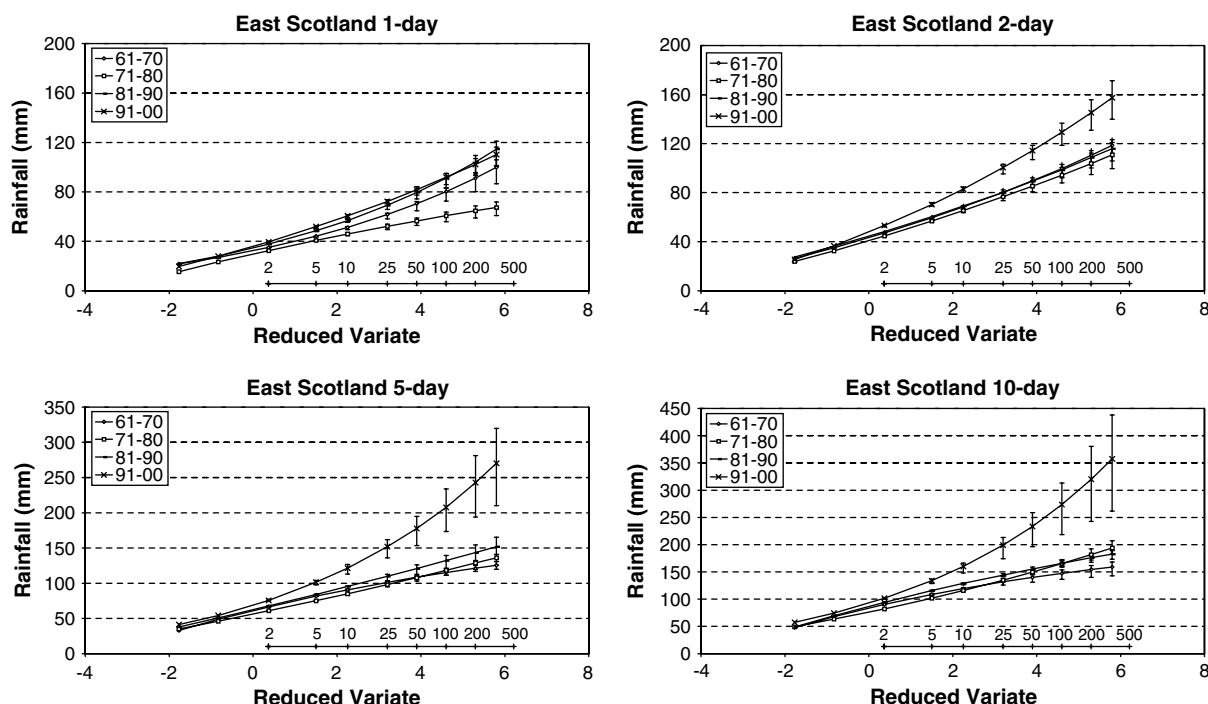Figure 9. Decadal change in RMED: (a) SWE 1-day; (b) NI 1-day; (c) SEE 1-day; (d) SEE 2-day

Figure 10. Decadal changes in return period estimates using mean regional RMED for the ES pooling region

In September 1995, the north and east of Scotland were the wettest regions of the UK (181 mm, 299% of normal in east Scotland) (Cullum, 1996). On the 7–8 September, 67 mm of rain fell at Aberdeen. This was followed by a further 70 mm at Glenlivet on the 9–10 September. A further depression tracked across the UK on the 10–11 September and Kinloss received 69 mm in 24 h on the 11–12 September. Repeated heavy downpours in northeast Scotland caused serious flooding along the southern shore of the Moray Firth and around Aberdeen. During the first 11 days of September 272 mm rain fell at Kinloss, for example, 13 times the normal for such a period. At Dyce the monthly total was 234 mm (344% of the 1961–90 average) (Weather Log, 1995).

In October 1993 there was widespread heavy rainfall and thunder over the first few days, caused by a complex low centred over England (Weather Log, 1993). At Dyce, the total for the month was 119 mm (145% of the 1961–90 average) and at Leuchars the total was 112 mm (198% of the 1961–90 average) (Weather Log, 1993).

There has also been a recent increase in extreme event occurrence in the pooling regions of SS, NS and NI, particularly at 5- and 10-day durations. The 10-day growth curves multiplied by regional mean *RMED* for NS and SS are shown in Figure 11(a) and (b) respectively. Here, however, the increase starts as early as the 1980s and is due to an increase in the magnitude of events (i.e. increasing *RMED*) rather than changes to the shape of the growth curve.

This increase is also seen in NEE and NWE for 5- and 10-day AM series. Figure 11(c) and (d) show the 10-day return period estimates for an average site in the NEE and NWE regions respectively. In the 1990s there has been an increase in long-duration, high-magnitude events, as shown by both the shape of the growth curve and increasing RMED.

5.5. Change in return period estimates

The above changes can be better seen in Table IV, which compares the 100-year event for 1961–90 with that of 1991–2000 for 5- and 10-day durations. In southern regions there is either little or negative change
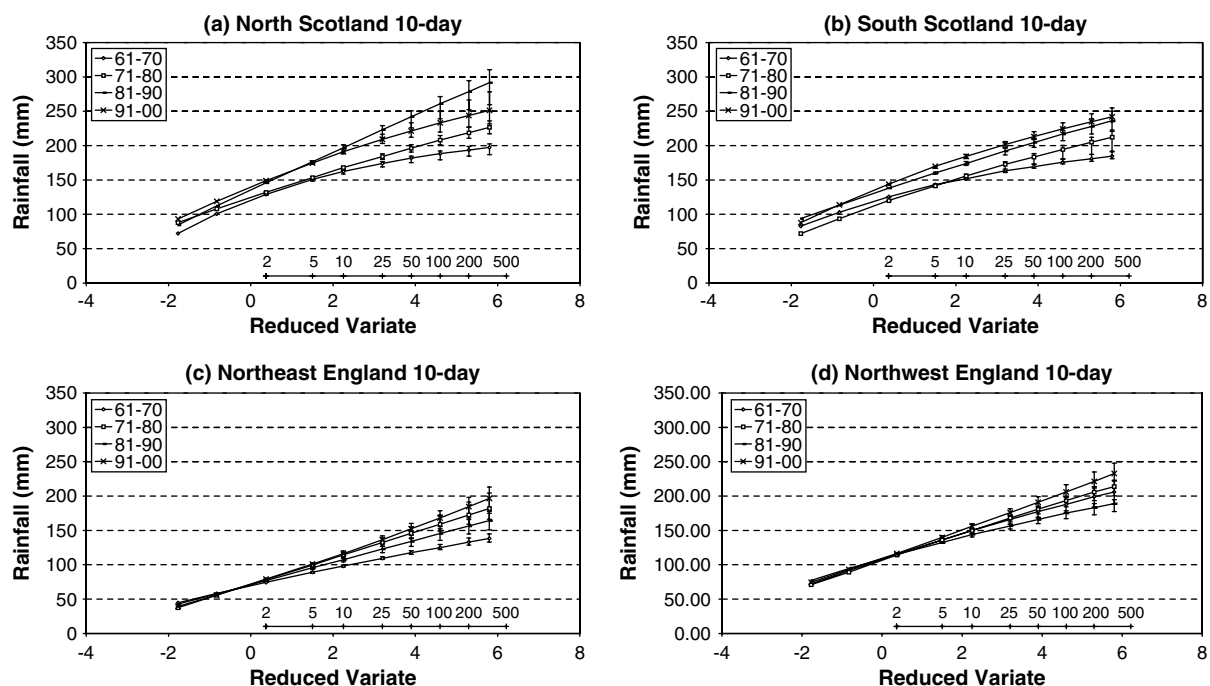
Figure 11. Decadal changes in 10-day duration return period estimates using mean regional RMED for: (a) NS; (b) SS; (c) NEE; (d) NWE

in the magnitude of the 100-year event. However, in northern pooling regions during the 1990s the 100-year event shows an increase in magnitude when compared with the 1961–90 average. This change is very prominent in ES, with a 75% increase in rainfall amount for the 100-year event. This may substantiate the recent move in Scotland to use the 200-year event for design and planning purposes (Fleming, 2001).

Another, and the more common, way of looking at this type of change is as a change in recurrence interval. Table V shows the change in average recurrence interval for a 50-year event for 5- and 10-day durations for the 1961–90 time period with the most recent decade from 1991 to 2000. It can be seen that the average recurrence interval has increased in southern pooling regions but decreased substantially in northern pooling regions. The 50-year event in Scotland during 1961–90 has become 8-year, 11-year and 25-year events in the ES, SS and NS pooling regions respectively during the 1990s. In northern England (NEE and NWE pooling regions) the average recurrence interval has also halved. This may have severe implications for design and planning practices for flood control.

6. DISCUSSION AND CONCLUSIONS

This study has shown that the frequency of extreme rainfall has changed over parts of the UK in the period 1961–2000. This may be due to natural climatic variability, climate change, or both. However, there are several caveats to the approach taken in this research, and these are discussed further here.

Firstly, although most procedures for rainfall frequency estimation are based on the analysis of AM series, this contradicts theoretical advice, which invariably recommends peak-over-threshold (POT) analysis. POT methods include all large events and exclude AM, which may be small and thus misleading in an extreme analysis. Unfortunately, however, the treatment of missing data in the POT approach is demanding, and determining which peaks to exclude during the same rainfall event can be very time consuming, so the AM series approach was adopted in the first instance.

Table IV. Change in the 100-year rainfall event for (a) 5-day and (b) 10-day durations for 1961–90 and 1991–2000. Italic indicates lower extremes in 1991–2000 than previously

Pooling region	Rainfall from the 100-year event (mm)		Change (%)
	(1961–90)	(1991–2000)	
(a)			
SWE	128	129	0
SEE	*123*	*104*	−15
CEE	105	106	2
NWE	148	160	9
NEE	115	130	13
NI	131	143	9
NS	159	171	8
SS	144	177	23
ES	122	208	71
(b)			
SWE	*175*	*160*	−8
SEE	*163*	*133*	−19
CEE	*127*	*123*	−3
NWE	185	206	11
NEE	143	168	18
NI	*161*	*158*	−2
NS	219	233	6
SS	196	224	15
ES	159	274	72

Secondly, no explicit account has been taken in this analysis of the spatial dependence of rainfall events between stations in a given region. It is clear, however, that some regions are affected by a single storm event giving rise to large totals at several sites. Many researchers have examined the problem of spatial dependence in the prediction of rainfall extremes (e.g. Hosking and Wallis, 1988; Dales and Reed, 1989). Dales and Reed (1989) account for spatial dependence by reducing the 'network' (pooling group) to an effective number of independent sites based on the number of sites in the network, area of the network and the duration of rainfall extremes. This allows the growth curve to be shifted a fixed distance to the right to account for spatial dependence. However, this method has not been extensively validated. Hosking and Wallis (1988) used a Monte Carlo simulation to assess the effect of realistically specified inter-site dependence on growth curve estimation in a regional frequency analysis. They found that: (a) any bias in quantile estimates is unchanged by the presence of inter-site dependence; (b) regional heterogeneity exerts a stronger effect on the growth curve than inter-site dependence; and, moreover (c) even when both heterogeneity and inter-site dependence are present, regional frequency analysis is more accurate than at-site analysis. Therefore, as a definitive methodology to account for spatial dependence is unavailable, this research relies on a bootstrap to estimate the likely error.

Thirdly, the assumption of 'quasi-stationarity' has been made in the decadal analysis. The selection of a 10 year period represents an arbitrarily chosen compromise between assuming stationarity and acquiring a larger data set to allow longer return periods to be estimated.

These assumptions aside, the major conclusions of this study are:

1. There have been significant but regionally varying changes in extreme rainfall event occurrence across the UK in the last 40 years.
2. Prolonged heavy rainfall events are increasing in northern and western regions. Growth curves have become steeper and annual maxima have increased during the 1990s due to both the growth curve changes and a

Table V. Probability of occurrence of the 1991–2000 (a) 5-day and (b) 10-day rainfall event corresponding to the 1961–90 50-year event

Pooling region	Probability of event (%)	Return period years
(a)		
SWE	2.2	45
SEE	0.6	167
CEE	2.9	35
NWE	3.4	30
NEE	3.9	26
NI	3.6	28
NS	3.5	28
SS	8.6	12
ES	13.5	7
(b)		
SWE	0.8	130
SEE	0.2	500
CEE	1.9	53
NWE	4.2	24
NEE	4.9	21
NI	2.4	42
NS	4.5	22
SS	9.2	11
ES	12.9	8

large increase in regional mean *RMED*. This is particularly evident in eastern Scotland, where the recent decade from 1991 to 2000 provides a significant departure from previous return-period estimates.
3. In the south (SEE, SWE and CEE) the growth curves have become flatter, and 5- and 10-day annual maxima have decreased during the 1990s, despite increasing *RMED* in most regions.

It has been shown that multi-day, prolonged heavy rainfall events are increasing in northern and western parts of the UK. These changes have implications for the design and maintenance of infrastructure, such as urban drainage systems and flood control measures. Return-period estimates presented here for different regions of the UK, using the most recent rainfall data, will allow the reassessment of the risk of failure of existing structures and facilitate the design of new structures incorporating better risk or uncertainty estimates.

A remaining issue is the question of what period of record should be used to formulate design standards in a transient climate. Many researchers have questioned the validity of giving equal weight to both historical and modern hydrometric data in return-period estimation (e.g. Marsh, 1996) given the changing pattern and increasing persistence of heavy rainfall events. For example, current practice is to rely on a climatological normal period such as 1961–90. FEH relies on historic data extending further back than 1961. There are strong indications from this work, and elsewhere, that changes have occurred in the 1980s and 1990s, which casts doubt on this approach. The alternatives are to use either a shorter period, such as 1991–2000, which may be more representative of future conditions, or to accommodate underlying non-stationarity in some way. Both of these approaches are fraught with uncertainties, and further research is needed to establish a robust approach that avoids the assumption of stationarity whilst using sufficient records to obtain reliable estimates.

7. FUTURE POSSIBILITIES

It is anticipated that the research presented in this paper will be built upon to examine the further possibilities of:

- Seasonal change in rainfall extremes (Fowler and Kilsby, 2003); this may be particularly important given the recent severe autumn flood events of 2000 and 2001 (Lamb, 2001), and notable changes in the seasonal distribution of rainfall quantiles shown by Osborn *et al.* (2000).
- Using POT data to produce revised growth curve estimates.
- Comparing the observed return-period estimates with those generated using an RCM, such as HadRM3, to develop a methodology that can produce accurate growth curves for the future climate given current information.
- Linking trends in rainfall extremes to trends in floods using various case studies.

REFERENCES

Bradley RS, Diaz HF, Eischeid JK, Jones PD, Kelly PM, Goodess CM. 1987. Precipitation fluctuations over Northern Hemisphere land areas since the mid-19th century. *Science* **237**: 171–275.

Brunetti M, Buffoni L, Maugeri M, Nanni T. 2000. Precipitation intensity trends in northern Italy. *International Journal of Climatology* **20**: 1017–1031.

Cullum D. 1996. Some features of Northern Hemisphere weather during autumn 1995. *Weather* **51**: 141–143.

Dales MY, Reed DW. 1989. Regional flood and storm hazard assessment. *Institute of Hydrology Rep. No. 102*. IH, Wallingford, UK.

Diaz HF, Bradley RS, Eischeid JK. 1989. Precipitation fluctuations over global land areas since the late 1800s. *Journal of Geophysical Research* **94**: 1195–1240.

Easterling DR, Meehl GA, Parmesan C, Changnon SA, Karl TR, Mearns LO. 2000. Climate extremes: observations, modeling, and impacts. *Science* **289**: 2068–2074.

Efron B. 1979. Bootstrap methods: another look at the jack-knife. *Annals of Statistics* **7**: 1–26.

Fleming G. 2001. Managing flood risk: past, present and future. In *Flood Risk in a Changing Climate*. Discussion Meeting at the Royal Society, London, 21–22 November, 2001.

Fowler HJ, Kilsby CG. 2003. Implications of changes in seasonal and annual extreme rainfall. *Geophysical Research Letters* **30**(13): 1720.

Frei C, Schar C. 2001. Detection probability of trends in rare events: theory and application to heavy precipitation in the alpine region. *Journal of Climate* **14**: 1568–1584.

Gringorten II. 1963. A plotting rule for extreme probability paper. *Journal of Geophysical Research* **68**: 813–814.

Groisman PY, Karl TR, Easterling DR, Knight RW, Jamason PF, Hennessy KJ, Suppiah R, Page CM, Wibig J, Fortuniak K, Razuvaev VN, Douglas A, Forland E, Zhai PM. 1999. Changes in the probability of heavy precipitation: important indicators of climatic change. *Climatic Change* **42**: 243–283.

Hennesey KJ, Gregory JM, Mitchell JF. 1997. Change in daily precipitation under enhanced greenhouse conditions. *Climate Dynamics* **13**: 667–680.

Hosking JRM. 1997. Fortran routines for use with the method of L-moments. Research Report RC 20525 (90933) Version 3.02. IBM Research Division, New York.

Hosking JRM, Wallis JR. 1988. The effect of intersite dependence on regional flood frequency analysis. *Water Resources Research* **24**: 588–600.

Hosking JRM, Wallis JR. 1997. *Regional Frequency Analysis: An Approach Based on L-Moments*. Cambridge University Press.

Hosking JRM, Wallis JR, Wood EF. 1985. Estimation of the generalised extreme-value distribution by the method of probability-weighted moments. *Technometrics* **27**: 251–261.

IH 1999. *Flood Estimation Handbook*. CEH Wallingford: Wallingford, UK.

Iwashima T, Yamamoto R. 1993. A statistical analysis of the extreme events: long-term trend of heavy daily precipitation. *Journal of the Meteorological Society of Japan* **71**: 637–640.

Jones PD, Reid PA. 2001. Assessing future changes in extreme precipitation over Britain using regional climate model integrations. *International Journal of Climatology* **21**: 1337–1356.

Karl TR, Knight RW. 1998. Secular trends of precipitation amount, frequency, and intensity in the United States. *Bulletin of the American Meteorological Society* **79**: 231–241.

Lamb R. 2001. To what extent can the October/November 2000 floods be attributed to climate change. DEFRA FD2304 Final Report.

Marsh TJ. 1996. The 1995 drought — a signal of climatic instability? *Proceedings of the Institution of Civil Engineers, Water, Maritime and Energy* **118**: 189–195.

Marsh TJ. 2001. The 2000/2001 floods in the UK — a brief overview. *Weather* **56**: 343–345.

McGuffie K, Henderson-Sellers A, Holbrook N, Kothavala Z, Balachova O, Hoekstra J. 1999. Assessing simulations of daily temperature and precipitation variability with global climate models for present and enhanced greenhouse climates. *International Journal of Climatology* **19**: 1–26.

Murphy JM, Mitchell JFB. 1995. Transient response of the Hadley Centre coupled ocean–atmosphere model to increasing carbon-dioxide. Part II: spatial and temporal structure of response. *Journal of Climate* **8**: 57–80.

NERC. 1975. *Flood Studies Report*. Institute of Hydrology: Wallingford, Oxford.

Osborn TJ, Hulme M, Jones PD, Basnett TA. 2000. Observed trends in the daily intensity of United Kingdom precipitation. *International Journal of Climatology* **20**: 347–364.

Palmer TN, Raisanen J. 2002. Quantifying the risk of extreme seasonal precipitation events in a changing climate. *Nature* **415**: 512–514.

Reed DW, Faulkner DS, Stewart EJ. 1999. The FORGEX method of rainfall growth estimation. II: description. *Hydrology and Earth System Sciences* **3**: 197–203.

Robson A, Reed D. 1999. *Flood Estimation Handbook. Volume 3. Statistical Procedures for Flood Frequency Estimation*. Institute of Hydrology: Wallingford.

Weather Log. 1993. October. Royal Meteorological Society publication.

Weather Log. 1995. September. Royal Meteorological Society publication.

Wigley TML, Lough JM, Jones PD. 1984. Spatial patterns of precipitation in England and Wales and a revised, homogenous England and Wales precipitation series. *Journal of Climatology* **4**: 1–25.

Zhai PM, Sun AJ, Ren FM, Liu XN, Gao B, Zhang Q. 1999. Chances of climate extremes in China. *Climatic Change* **42**: 203–218.